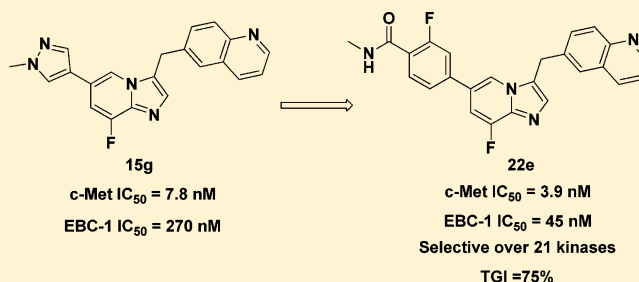


Design, Synthesis, and Biological Evaluation of Novel Imidazo[1,2-*a*]pyridine Derivatives as Potent c-Met InhibitorsChunpu Li,^{†,||} Jing Ai,^{‡,||} Dengyou Zhang,^{†,||} Xia Peng,[‡] Xi Chen,[†] Zhiwei Gao,[§] Yi Su,[‡] Wei Zhu,[†] Yinchun Ji,[‡] Xiaoyan Chen,[§] Meiyu Geng,^{*,‡} and Hong Liu^{*,†}[†]CAS Key Laboratory of Receptor Research, and [‡]Division of Anti-Tumor Pharmacology, Shanghai Institute of Materia Medica, Chinese Academy of Sciences, 555 Zu Chong Zhi Road, Shanghai 201203, P. R. China[§]Shanghai Institute of Materia Medica, Chinese Academy of Sciences, 501 Haike Road, Shanghai 201203, P. R. China

Supporting Information

ABSTRACT: A series of imidazo[1,2-*a*]pyridine derivatives against c-Met was designed by means of bioisosteric replacement. In this study, a selective, potent c-Met inhibitor, **22e** was identified, with IC₅₀ values of 3.9 nM against c-Met kinase and 45.0 nM against c-Met-addicted EBC-1 cell proliferation, respectively. Compound **22e** inhibited c-Met phosphorylation and downstream signaling across different oncogenic forms in c-Met overactivated cancer cells and model cells. Compound **22e** significantly inhibited tumor growth (TGI = 75%) with good oral bioavailability (*F* = 29%) and no significant hERG inhibition. On the basis of systematic metabolic study, the pathway of all possible metabolites of **22e** in liver microsomes of different species has been proposed, and a major NADPH-dependent metabolite **33** was generated by liver microsomes. To block the metabolic site, **42** was designed and synthesized for further evaluation. Taken together, the imidazo[1,2-*a*]pyridine scaffold showed promising pharmacological inhibition of c-Met and warrants further investigation.

KEYWORDS: Receptor tyrosine kinase, c-Met inhibitor, imidazo[1,2-*a*]pyridine, metabolic stability



Receptor tyrosine kinases (RTKs) have a critical role in the development and progression of many types of cancer.¹ The receptor tyrosine kinase c-Met is expressed mainly by epithelial cells of many organs.² Activation of c-Met is regulated upon binding with its natural ligand, hepatocyte growth factor (HGF),³ and interaction with other membrane receptors.⁴ The normal functions of HGF/c-Met pathway are largely restricted to embryogenesis, tissue injury repair, and regeneration in adults.⁵ Dysregulation of the HGF/c-Met pathway (through, e.g., c-Met transcriptional upregulation, *MET* gene amplification or rearrangement, and activating mutations of *MET* gene) can induce cell proliferation, invasion, migration, and apoptosis avoidance, leading to tumor growth, angiogenesis, and metastasis.³ Importantly, aberrant c-Met activation observed frequently in many human solid tumors and hematological malignancies is associated with poor clinical outcomes.⁶ Furthermore, overactivation of c-Met causes therapeutic resistance.⁷ For these reasons, c-Met has become an attractive target for cancer therapy.

Recently, a numerous number of small molecule c-Met inhibitors have been reported (Figure 1). Compound **1** (Crizotinib)⁸ developed by Pfizer is a potent c-Met/ALK dual inhibitor, which demonstrated marked efficacy for a subset of nonsmall cell lung cancer (NSCLC) patients with an EML4-ALK fusion gene. Phase I clinical trial of inhibitor **2** (JNJ38877605)⁹ has been terminated because of an increase in serum creatinine levels. Inhibitor **3** (SGX-523) is no longer

in clinical development because of acute renal failure.¹⁰ Without any safety concerns, the clinical study of inhibitor **4** (PF-04217903)¹¹ was prematurely discontinued. In addition, compounds **5** (AMG-337)¹² and **6** (INC-280)¹³ were reported and have entered phase II clinical trials.

Among the known c-Met inhibitors, bicyclic triazole-based or triazine-based inhibitors demonstrated high c-Met inhibitory potency and excellent selectivity against other kinases. However, many projects of these inhibitors in clinical or discovery development were stopped due to toxicity or unknown reasons.^{9,10,14} Thus, there is still a need to discover new classes of inhibitors against c-Met for the treatment of cancer patients. The publicly available cocrystal structure of PF-04217903 within c-Met (PDB 3ZXZ) disclosed the binding mode of this kind of inhibitors.¹¹ Generally, the quinoline nitrogen atom participates in a hydrogen bond with the hinge region residue Met-1160. The N-3 nitrogen of triazolopyrazine backbone formed a hydrogen bond with Asp-1222. Meanwhile, triazolopyrazine backbone plays an important role in both c-Met activity and kinase selectivity via the unique face-to-face π -stacking interaction with the activation loop residue Tyr-1230, and there is a positive correlation between electron deficiency

Received: November 25, 2014

Accepted: March 1, 2015

Published: March 2, 2015

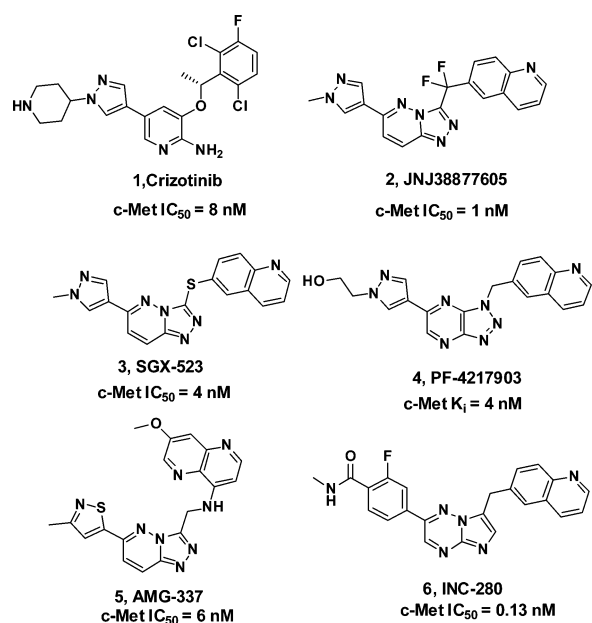


Figure 1. Representative c-Met inhibitors.

of bicyclic aromatic rings and the strength of π - π interaction with Tyr-1230.¹¹ The substituted aryl/heteroaryl (e.g., 1-methylpyrazole) on the backbone reaches out into the solvent (Figure 2). Bioisosteric replacement is a powerful method for

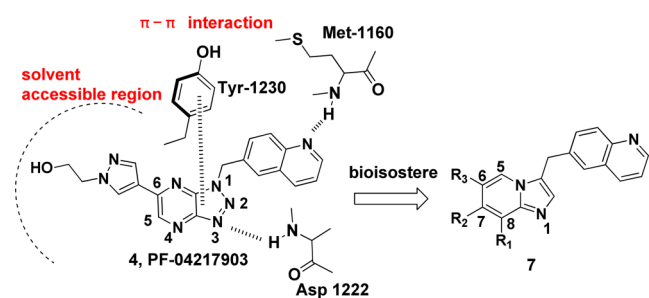


Figure 2. Design of the imidazo[1,2-*a*]pyridine scaffold.

the identification of novel chemical series in medicinal chemistry. On the basis of the previous work by Merck, 8-fluoroimidazo[1,2-*a*]pyridine has been established as a physicochemical mimic of imidazo[1,2-*a*]pyrimidine, using both in silico and traditional techniques.¹⁵ To the best of our knowledge, there are still no examples of using this strategy to discover novel c-Met inhibitors. Hence, we tried to replace the 8-position N atom with a C-F bond to mimic the properties of N-8 atom, including electrostatic surface and lipophilicity to keep the electron deficiency of bicyclic aromatic rings. Meanwhile, we tried to introduce Cl, CN, and CF₃ on the imidazo[1,2-*a*]pyridine to evaluate the influence of the electron density of bicyclic aromatic rings on c-Met inhibition. On the basis of the cocrystal structural information and principles of bioisosterism, we designed a novel imidazo[1,2-*a*]pyridine scaffold as c-Met inhibitors. Herein, we describe our recent effort on the synthesis and SARs of this series of compounds.

To achieve a structure-activity relationship (SAR) exploration, efficient synthetic routes were employed for preparation of the analogues (Schemes 1 and 2 in Supporting Information).

These novel imidazo[1,2-*a*]pyridine derivatives against c-Met have not been previously synthesized and evaluated; therefore,

the initial goal was to identify the optimal substituent. To identify potent c-Met inhibitors efficiently, we initially selected 1-methylpyrazole as a substituent at the C-6 position while varying the C-7 and C-8 substituents (Table 1). The initial

Table 1. SAR of Substituents on the Imidazo[1,2-*a*]pyridine Scaffold

Compd	R ₁	R ₂	R ₃	IC ₅₀ (nM) ^a	EBC-1 ^b IC ₅₀ (μM)
15a	Cl	H	CH ₃	2180±120	ND ^c
15b	H	Cl	CH ₃	24.5% @ 1 μM	ND
15c	CF ₃	H	CH ₃	9.6% @ 1 μM	ND
15d	H	CF ₃	CH ₃	5.9% @ 1 μM	ND
15e	CN	H	CH ₃	34.5% @ 100 μM	ND
15f	H	CN	CH ₃	33.3% @ 100 μM	ND
15g	F	H	CH ₃	7.8±0.3	0.27±0.05
15h	F	H	HO-CH ₂ -CH ₂ -*	3.2±0.3	0.34±0.03
15i	F	H	HN(CH ₂) ₂ -*	11.1±1.7	1.46±0.02

^aIC₅₀ values were calculated by the Logit method from the results of at least two independent tests with eight concentrations each and expressed as mean ± SD; c-Met IC₅₀ of Crizotinib = 2.4 ± 0.1 nM; c-Met IC₅₀ of JNJ38877605 = 1.8 ± 0.3 nM. ^bEBC-1: human nonsmall-cell lung cancer cell line that expresses elevated levels of constitutively active c-Met. ^cNot detected.

biochemical assay found that compound 15a exhibited moderate activity with an enzymatic IC₅₀ of 2.18 μM against c-Met. The activity did not significantly change with the introduction of different substituents at the C-7 or C-8 position (15b–15f). To our delight, compound 15g exhibited c-Met inhibition with an enzymatic IC₅₀ of 7.8 nM and an EBC-1 cell IC₅₀ of 0.27 μM, respectively. These encouraging results prompted us to investigate the SAR for substituents on the pyrazole while keeping the fluorine substitute at the C-8 position. The incorporation of polar groups, such as an ethanolic group (15h) and a piperidine group (15i) on the pyrazole of 15g resulted in 1.2-fold and 5.4-fold loss of cellular potency, respectively.

To gain structural information for further optimization, the 3D proposed binding modes of representative compounds 15a, 15c, 15e, and 15g were generated by docking simulation (Figure 3). For each compound, the best pose with the lowest binding energy was selected for further analysis with Glide¹⁶ and PyMOL.¹⁷ The binding mode indicated that compound 15g was bound to the active site of c-Met, similar to PF-04217903 (Figure 3A). The nitrogen of quinoline H-bonds well with the hinge region Met-1160, whereas the N-1 nitrogen of the imidazo[1,2-*a*]pyridine scaffold formed a hydrogen bond with Asp-1222. In addition, imidazo[1,2-*a*]pyridine core kept a π - π interaction with electron rich Tyr-1230, which is critical for c-Met inhibition. Compared with 15g, the binding pose of 15c (Figure 3B) was entirely different since the bulky C-8 CF₃ substituent could not enter the inside pocket, which could be the main reason for the loss in inhibitory activity. Compared

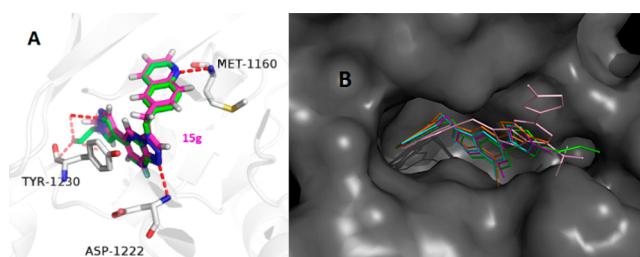


Figure 3. Binding model comparison of designed compounds with PF-04217903. (A) Binding pose of compound **15g** (purple) and PF-04217903 (green) with c-Met. (B) Overlay of **15a** (blue), **15c** (pink), **15e** (orange), and **15g** (purple) in the same cavity along with PF-04217903 (green) as the reference molecule.

with 8-fluoroimidazo[1,2-*a*]pyridine core (**15g**), the 8-chloroimidazo[1,2-*a*]pyridine is more electron-rich, leading to a decreased interaction with Tyr-1230. Taken together, these results could give an explanation to the different inhibition of these compounds.

Subsequently, the SAR at the 6-position of the imidazo[1,2-*a*]pyridine scaffold was investigated (Table 2). Introduction of heteroaryl substituents (**16a–c**) displayed good c-Met inhibition. The pyridinyl analogue **16b**, which incorporated a cyano group, was more effective, and the EBC-1 cell IC_{50} reached to 188.5 nM. Among the phenyl derivatives (**16d–g**), benzonitrile analogues **16d** and **16f** demonstrated improved c-Met inhibition, with an EBC-1 cell IC_{50} of 106.7 and 145.0 nM, respectively. These observations indicated that incorporation of polar groups on 6-phenyl had a significant influence on cellular activity. Encouraged by these results, analogues incorporated by polar amide groups on 6-phenyl were prepared for SAR exploration. 6-Benzamide analogue **22a** displayed 4-fold loss in cellular activity compared with **16d**. Derivatives bearing 4-fluoro-3-*N*-methylbenzamide (**22b**) and 4-chloro-3-*N*-methylbenzamide (**22c**) groups displayed less potent c-Met inhibition than **22a**. However, derivatives bearing 3-methoxy-4-*N*-methylbenzamide (**22d**) and 3-fluoro-4-*N*-methylbenzamide (**22e**) groups exhibited remarkably improved cellular activity. In particular, compound **22e** showed an enzymatic IC_{50} of 3.9 nM and good EBC-1 cell IC_{50} of 45.0 nM. These results indicated that the 3-F and 3-OMe might be important for c-Met inhibition.

To further modulate physical chemical properties of these inhibitors, substituted amides were introduced, especially amides with polar groups such as basic amines on their *N*-terminus (Table 3). First, the *N,N'*-disubstituted amide analogues were evaluated. Compounds **22f** and **22g** showed an EBC-1 cell IC_{50} of 405.5 and 868.9 nM, respectively, suggesting that *N*-monosubstituents were preferred here. Next, we investigated the influence of monosubstitution of the *N*-terminus of the amide on c-Met inhibition. For example, compound **22h**, which contained a morpholinoethyl group on the *N*-terminus of the amide, demonstrated c-Met inhibition by 2-fold compared with **22e**, and there was no significant differences between their EBC-1 activity. Replacement of the morpholinoethyl group with a noncyclic dimethylaminoethyl group (compound **22i**, enzymatic IC_{50} = 2.4 nM and EBC-1 cell IC_{50} = 49 nM) slightly improved the cell inhibitory activity. Compound **22j**, with a longer C-chain of the amide, reduced EBC-1 cell inhibitory activity by 3-fold. We also investigated the SARs of the compounds by restricting the side-chain conformation at the *N*-terminus of the amides (compounds

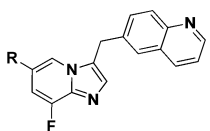
Table 2. SAR at the 6-Position of the Imidazo[1,2-*a*]pyridine Scaffold

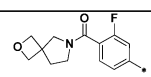
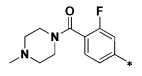
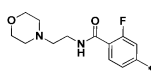
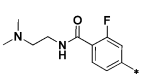
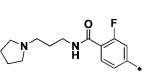
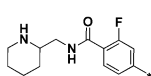
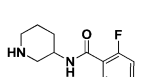
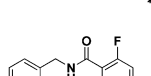
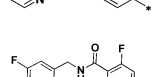
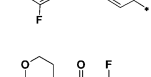
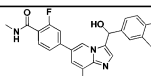
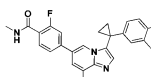
Compd	R	IC_{50} (nM) ^a	EBC-1 ^b IC_{50} (nM)
16a		4.3±0.6	443.6±6.9
16b		5.6±1.9	188.5±23.3
16c		14.5±0.2	224.6±75.1
16d		1.8±0.3	106.7±15.3
16e		2.7±0.4	790.1±194.1
16f		3.3±0.2	145.0±39.2
16g		2.8±0.5	407.4±164.0
16h		9.7±0.7	1475.0±260.0
22a		6.0±0.9	400.0±159.5
22b		16.2±1.6	246.4±86.3
22c		12.8±0.2	946.4±322.4
22d		10.6±0.2	59.6±17.7
22e		3.9±0.7	45.0±12.7

^a IC_{50} values were calculated by the Logit method from the results of at least two independent tests with eight concentrations each and expressed as mean ± SD; c-Met IC_{50} of Crizotinib = 2.4 ± 0.1 nM; c-Met IC_{50} of JNJ38877605 = 1.8 ± 0.3 nM. ^bEBC-1: human nonsmall-cell lung cancer cell line that expresses elevated levels of constitutively active c-Met.

22k, **22l**, and **22o**). When the *N*-terminus of the amide was replaced with a piperidin-2-ylmethyl group (compound **22k**, EBC cell IC_{50} = 276.8 nM) or a piperidin-3-yl group (compound **22l**, EBC cell IC_{50} = 137.5 nM), c-Met inhibition was 5.5- and 4.3-fold more potent than **22e**, respectively. In addition, we investigated compounds that contained an aryl group or a heteroaryl group on the *N*-terminal side of the amides. Compound **22m** showed sharply decreased c-Met cell inhibition, which could be caused by an intramolecular hydrogen bond interaction between the hydrogen atom of

Table 3. SAR of Substituents on the Amides



Compd	R	IC ₅₀ (nM) ^a	EBC-1 ^b IC ₅₀ (nM)
22f		21.4±2.0	405.5±155.6
22g		39.1±3.4	868.9±22.8
22h		2.0±0.3	52.0±15.6
22i		2.4±0.1	49.0±19.4
22j		3.4±1.1	161.3±2.2
22k		0.7±0.2	276.8±0.7
22l		0.9±0.3	137.5±1.3
22m		8.3±1.6	5549.9±839.2
22n		4.7±0.1	53.6±18.7
22o		4.2±0.7	70.5±37.5
Compd	Structure	IC ₅₀ (nM)	EBC-1 ^b IC ₅₀ (nM)
33		82.9 ± 25.9	3022.3 ± 432.8
42		23.5 ± 4.6	60.0 ± 7.2

^aIC₅₀ values were calculated by the Logit method from the results of at least two independent tests with eight concentrations each and expressed as mean ± SD; c-Met IC₅₀ of Crizotinib = 2.4 ± 0.1 nM; c-Met IC₅₀ of JNJ38877605 = 1.8 ± 0.3 nM. ^bEBC-1: human non-small-cell lung cancer cell line that expresses elevated levels of constitutively active c-Met.

the amide and the pyridine nitrogen. The potency of compound **22n** against EBC-1 cell proliferation is comparable to that of optimal compound **22e**.

Given its promising enzymatic and cellular potency, **22e** was selected as the lead compound for subsequent evaluation. In contrast to its high potency against c-Met, **22e** had barely any inhibitory effect on the other 21 tested kinases, including c-Met family member RON and highly homologous kinases Axl, c-Mer, and Tyro-3 (IC₅₀ > 10 μM), indicating that **22e** was a selective c-Met inhibitor (Table S1 in Supporting Information).

As shown in Figure S1 (See Supporting Information), **22e** inhibited the phosphorylation of c-Met and its key downstream molecules Akt and Erk in a dose-dependent manner in representative cancer or model cell lines (EBC-1, MKN45, and BaF3/TPR-Met cells). These results suggested that **22e** suppressed c-Met signaling across different oncogenic forms in c-Met overactivated cells.

Compound **22e** significantly inhibited cell proliferation of EBC-1, MKN-45, SNU-5, and BaF3/TPR-Met cells, which are characterized by a c-Met-dependent cell growth, with an IC₅₀ value of 45.0 to 203.2 nM (Table 4); however, **22e** barely

Table 4. Effects of **22e** on Cell Proliferation

IC ₅₀ (nM) ^a	22e	JNJ38877605	Crizotinib
EBC-1	45.0 ± 12.7	9.5 ± 2.0	21.8 ± 6.5
MKN-45	90.9 ± 17.4	10.9 ± 0.4	38.1 ± 8.8
SNU-5	70.2 ± 19.6	15.8 ± 3.2	20.4 ± 14.4
BaF3/TPR-Met	203.2 ± 4.4	17.6 ± 2.2	127.4 ± 8.1

^aThe IC₅₀ values are shown as the mean ± SD (nM) from three separate experiments.

inhibited these other cell lines, of which had Met low expression or activation (IC₅₀ > 50 μM) (Figure S2A in Supporting Information). c-Met inhibition blocks cell proliferation via arresting cells in G1/S phase.¹⁸ Compound **22e** induced a G1/S phase arrest in the EBC-1 cells, with 81.84% of the cell population in G1 phase in the presence of 1 μM **22e** (versus 52.95% in the vehicle control group) (Figure S2B,C in Supporting Information).

The HGF/c-Met axis activation promotes cell invasion and migration to allow cancer metastasis.¹⁹ Compound **22e** inhibited the migration of HGF-induced NCI-H441 cells, and almost completely blocked the cell migration phenotype at a dose of 500 nM (Figures S3A,C in Supporting Information). Further, **22e** strongly suppressed the invasion of HGF-induced NCI-H441 cell (Figures S3B,D in Supporting Information).

Cell scattering induced by HGF/c-Met activation is a hallmark of cancer invasiveness and metastasis.²⁰ Upon HGF stimulation, epithelial cells undergo colony dispersal and become migratory, fibroblast-like cells.²¹ Compound **22e** treatment reduced HGF-induced cell scattering of MDCK canine kidney epithelial cells in a dose-dependent manner (Figures S4 in Supporting Information). Collectively, these results indicated that **22e** inhibited the metastasis and invasiveness phenotype evoked by the HGF/c-Met axis in cancer.

Upon HGF stimulation, c-Met induces several biological responses that collectively give rise to a program known as invasive growth, which is pivotal to drive cancer cell invasion and metastasis.²² Thus, we investigated whether **22e** inhibited c-Met-mediated invasive growth. Exposure to **22e** inhibited branching morphogenesis in MDCK cells (Figures S5 in Supporting Information), indicating the **22e** inhibited HGF-induced c-MET-mediated invasive growth.

The pharmacokinetic (PK) profiles of the selected compound **22e** were assessed in Sprague–Dawley (SD) rats (Table S2 in Supporting Information). Compound **22e** showed a high area under the curve (AUC_{0-∞}) when dosed orally. The half-life and the absolute oral bioavailability of compound **22e** were 1.17 h and 29.4%, respectively.

We used the ultraperformance liquid chromatography quadrupole time-of-flight mass spectrometry (UPLC-qTOF-MS) method to identify the possible metabolites of **22e** in liver microsomes of different species. We have proposed the metabolism pathway and all the metabolites of **22e** (Scheme 3a in Supporting Information). In view of the result that the major oxidant metabolism take place in the benzyl position of this scaffold, we speculated that metabolite **33** was the major metabolite of **22e** after incubation in mice, dog, monkey, and human liver microsomes, except rat liver microsomes (Table S3 in Supporting Information).

The IC₅₀ value of compound **22e** on hERG was 93.56 μM using a FluxOR thallium assay. Thus, **22e** did not show significant hERG inhibition.

To assess the *in vivo* antitumor efficacy of **22e**, an EBC-1 xenograft model specifically driven by *MET* amplification was chosen. After 21 days of **22e** (methanesulfonic salt) oral administration, dose-dependent tumor growth inhibition was observed in **22e** treated groups, with an inhibitory rate of 75.0% (*P* < 0.05) and 62.9% (*P* < 0.05) at doses of 100 and 50 mg/kg, respectively (Figure 4). No significant weight losses were observed (data not shown).

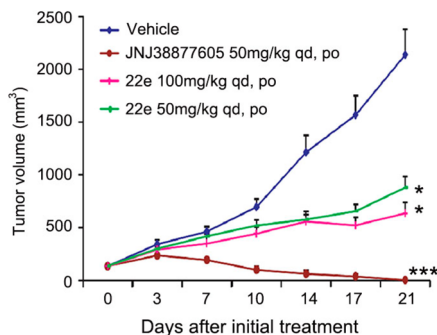


Figure 4. Compound **22e** inhibits tumor growth in EBC-1 xenografts. Compound **22e** in the methanesulfonic acid salt form or JNJ38877605 was administered orally once daily for 3 weeks after the tumor volume reached 100 to 150 mm³. The results are expressed as the mean ± SEM (drug-treated group, *n* = 6; vehicle group, *n* = 12). **p* < 0.05, ****p* < 0.001 vs control group, determined using Student's *t* test.

Furthermore, we synthesized the major metabolite **33** for investigation (Scheme 3b in Supporting Information); however, it had no significant inhibitory effect on c-Met-dependent cell proliferation (enzymatic IC₅₀ = 82.9 ± 25.9 nM and EBC-1 cell IC₅₀ = 3022.3 nM). Since we have identified metabolic hot spots of **22e**, we designed and synthesized compound **42** (Scheme 4 in Supporting Information), which bears a cyclopropyl at the linker of this scaffold that might block the metabolic site.²³ Even though **42** demonstrated potent inhibitory effect on c-Met kinase and c-Met-dependent cell viability (enzymatic IC₅₀ = 23.5 nM and EBC-1 cell IC₅₀ = 60.0 nM), the *in vivo* antitumor efficacy of **42** was disappointing. Further optimization to improve the metabolic stability and *in vivo* antitumor efficacy are ongoing in our laboratory.

In conclusion, a series of novel imidazo[1,2-*a*]pyridine derivatives were designed, synthesized, and evaluated as c-Met inhibitors by means of bioisosteric replacement. SAR exploration led to the identification of a potent, selective c-Met inhibitor **22e**. Compound **22e** showed strong potency against c-Met kinase and inhibited c-Met phosphorylation and downstream signaling across different oncogenic forms in c-Met overactivated cancer cells and model cells. Furthermore, **22e** treatment resulted in significant antitumor activity in c-Met-driven EBC-1 xenografts. Compound **42** was designed by means of metabolite identification. Further optimizations are currently under investigation.

■ ASSOCIATED CONTENT

📄 Supporting Information

Synthetic procedures and analytical data for compounds reported in this letter and procedures for *in vitro* and *in vivo* assays. This material is available free of charge via the Internet at <http://pubs.acs.org>.

■ AUTHOR INFORMATION

Corresponding Authors

*(M.G.) E-mail: mygeng@simm.ac.cn. Phone: +86-21-50806600-2426.

*(H.L.) E-mail: hliu@simm.ac.cn. Phone: +86-21-50807042.

Author Contributions

†C.L., J.A., and D.Z. contributed equally to this work.

Funding

We gratefully acknowledge financial support from the National Natural Science Foundation of China (Grants 91229204 and 81220108025), Major Project of Chinese National Programs for Fundamental Research and Development (2015CB910304), National High Technology Research and Development Program of China (2012AA020302), National Basic Research Program of China (2012CB518005), and National ST Major Projects (2012ZX09103101-072, 2014ZX09507002-001, and 2013ZX09507-001).

Notes

The authors declare no competing financial interest.

■ ABBREVIATIONS

c-Met, mesenchymal-epithelial transition factor; ALK, anaplastic lymphoma kinase; SARs, structure–activity relationships; AUC, area under curve

■ REFERENCES

- Zwick, E.; Bange, J.; Ullrich, A. Receptor tyrosine kinase signalling as a target for cancer intervention strategies. *Endocr. Relat. Cancer* **2001**, *8*, 161–173.
- Trusolino, L.; Comoglio, P. M. Scatter-factor and semaphorin receptors: cell signalling for invasive growth. *Nat. Rev. Cancer* **2002**, *2*, 289–300.
- Bottaro, D. P.; Rubin, J. S.; Faletto, D. L.; Chan, A. M.; Kmieciak, T. E.; Vande Woude, G. F.; Aaronson, S. A. Identification of the hepatocyte growth factor receptor as the c-met proto-oncogene product. *Science* **1991**, *251*, 802–804.
- Garouniatis, A.; Zizi-Sermpetzoglou, A.; Rizos, S.; Kostakis, A.; Nikiteas, N.; Papavassiliou, A. G. Vascular endothelial growth factor receptors 1,3 and caveolin-1 are implicated in colorectal cancer aggressiveness and prognosis—correlations with epidermal growth factor receptor, CD44v6, focal adhesion kinase, and c-Met. *Tumour Biol.* **2013**, *34*, 2109–2117.

(5) Porter, J. Small molecule c-Met kinase inhibitors: a review of recent patents. *Expert Opin. Ther. Pat.* **2010**, *20*, 159–177.

(6) Parr, C.; Watkins, G.; Mansel, R. E.; Jiang, W. G. The hepatocyte growth factor regulatory factors in human breast cancer. *Clin. Cancer Res.* **2004**, *10*, 202–211.

(7) Engelman, J. A.; Zejnullahu, K.; Mitsudomi, T.; Song, Y.; Hyland, C.; Park, J. O.; Lindeman, N.; Gale, C. M.; Zhao, X.; Christensen, J.; Kosaka, T.; Holmes, A. J.; Rogers, A. M.; Cappuzzo, F.; Mok, T.; Lee, C.; Johnson, B. E.; Cantley, L. C.; Janne, P. A. MET amplification leads to gefitinib resistance in lung cancer by activating ERBB3 signaling. *Science* **2007**, *316*, 1039–1043.

(8) Cui, J. J.; Tran-Dube, M.; Shen, H.; Nambu, M.; Kung, P. P.; Pairish, M.; Jia, L.; Meng, J.; Funk, L.; Botrous, I.; McTigue, M.; Grodsky, N.; Ryan, K.; Padrique, E.; Alton, G.; Timofeevski, S.; Yamazaki, S.; Li, Q.; Zou, H.; Christensen, J.; Mroczkowski, B.; Bender, S.; Kania, R. S.; Edwards, M. P. Structure based drug design of crizotinib (PF-02341066), a potent and selective dual inhibitor of mesenchymal-epithelial transition factor (c-MET) kinase and anaplastic lymphoma kinase (ALK). *J. Med. Chem.* **2011**, *54*, 6342–6363.

(9) Clinical trial data: <https://www.clinicaltrials.gov/ct2/show/NCT00651365>.

(10) Diamond, S.; Boer, J.; Maduskuie, T. P., Jr.; Falahatpisheh, N.; Li, Y.; Yeleswaram, S. Species-specific metabolism of SGX523 by aldehyde oxidase and the toxicological implications. *Drug Metab. Dispos.* **2010**, *38*, 1277–1285.

(11) Cui, J. J.; McTigue, M.; Nambu, M.; Tran-Dube, M.; Pairish, M.; Shen, H.; Jia, L.; Cheng, H.; Hoffman, J.; Le, P.; Jalaie, M.; Goetz, G. H.; Ryan, K.; Grodsky, N.; Deng, Y. L.; Parker, M.; Timofeevski, S.; Murray, B. W.; Yamazaki, S.; Aguirre, S.; Li, Q.; Zou, H.; Christensen, J. Discovery of a novel class of exquisitely selective mesenchymal-epithelial transition factor (c-MET) protein kinase inhibitors and identification of the clinical candidate 2-(4-(1-(quinolin-6-ylmethyl)-1H-[1,2,3]triazolo[4,5-b]pyrazin-6-yl)-1H-pyrazol-1-yl)ethanol (PF-04217903) for the treatment of cancer. *J. Med. Chem.* **2012**, *55*, 8091–8109.

(12) Clinical trial data: <https://www.clinicaltrials.gov/ct2/show/NCT02016534>.

(13) Clinical trial data: <https://www.clinicaltrials.gov/ct2/show/NCT01737827>.

(14) Clinical trial data: <https://www.clinicaltrials.gov/ct2/show/NCT00706355>.

(15) Humphries, A. C.; Gancia, E.; Gilligan, M. T.; Goodacre, S.; Hallett, D.; Merchant, K. J.; Thomas, S. R. 8-Fluoroimidazo[1,2-*a*]pyridine: synthesis, physicochemical properties and evaluation as a bioisosteric replacement for imidazo[1,2-*a*]pyrimidine in an allosteric modulator ligand of the GABA A receptor. *Bioorg. Med. Chem. Lett.* **2006**, *16*, 1518–1522.

(16) Glide, version 5.5, Schrödinger, LLC, New York, NY, 2009.

(17) PyMOL, Version 1.4.1, Schrödinger, LLC, New York, NY, 2011.

(18) Bertotti, A.; Burbidge, M. F.; Gastaldi, S.; Galimi, F.; Torti, D.; Medico, E.; Giordano, S.; Corso, S.; Rolland-Valognes, G.; Lockhart, B. P.; Hickman, J. A.; Comoglio, P. M.; Trusolino, L. Only a subset of Met-activated pathways are required to sustain oncogene addiction. *Sci. Signaling* **2009**, *2*, ra80.

(19) Jeffers, M.; Rong, S.; Vande Woude, G. F. Hepatocyte growth factor/scatter factor-Met signaling in tumorigenicity and invasion/metastasis. *J. Mol. Med.* **1996**, *74*, 505–513.

(20) Stoker, M.; Gherardi, E.; Perryman, M.; Gray, J. Scatter factor is a fibroblast-derived modulator of epithelial cell mobility. *Nature* **1987**, *327*, 239–242.

(21) Thiery, J. P. Epithelial-mesenchymal transitions in tumour progression. *Nat. Rev. Cancer* **2002**, *2*, 442–54.

(22) Gherardi, E.; Birchmeier, W.; Birchmeier, C.; Vande Woude, G.; Targeting, M. E. T. in cancer: rationale and progress. *Nat. Rev. Cancer* **2012**, *12*, 89–103.

(23) Zhou, J.; Metcalf, B.; Xu, M.; He, C.; Zhang, C.; Qian, D.; Burns, D. M.; Li, Y.; Yao, W. Imidazotriazines and Imidazopyrimidines as kinase inhibitors. PCT Int. Appl. WO 2008/064157A1, 2008.